

SPIN EFFECTS IN  $\tau$  LEPTON PAIR PRODUCTION  
AT LHC\*T. PIERZCHAŁA<sup>a</sup>, E. RICHTER-WĄS<sup>b,c,d</sup>, Z. WĄS<sup>d,e</sup> AND M. WOREK<sup>a</sup><sup>a</sup>Institute of Physics, University of Silesia  
Uniwersytecka 4, 40-007 Katowice, Poland<sup>b</sup>Institute of Computer Science, Jagellonian University  
Nawojki 11, 30-072 Cracow, Poland<sup>c</sup>CERN, PPE, 1211 Geneva 23, Switzerland<sup>d</sup>Institute of Nuclear Physics

Kawory 26a, 30-055 Cracow, Poland

<sup>e</sup>CERN, Theory Division, 1211 Geneva 23, Switzerland*(Received January 25, 2001)*

The proper incorporation of spin effects in  $\tau$  lepton decays is often of importance. In the present work the case of the  $Z/\gamma \rightarrow \tau^+\tau^-$  production mechanism is studied in detail. As an example, the effects due to the spin correlations on the potential for the Minimal Supersymmetric Standard Model (MSSM) Higgs boson(s) searches in the  $\tau\tau$  decay channel at the Large Hadron Collider (LHC) are discussed. For these processes, the Standard Model  $Z/\gamma^* \rightarrow \tau\tau$ -pair production is a dominant background. The spin effects in high energy physics reactions, can be implemented up to certain approximation, independently of the algorithm and matrix elements used by the production program. Information stored on every generated event can be sufficient. The algorithm based on such approximation is documented. Question of the theoretical uncertainty is partly discussed.

PACS numbers: 14.60.Fg

**1. Introduction**

In a study of “discovery potential” and data analysis of present high energy experiments the problems of precise predictions including, simultaneously, signal signatures of the new (or studied) physics, backgrounds, as well as all detector related effects should be analysed. It is generally believed that a Monte Carlo simulation of the full chain from the beam collision to detector response is the most convenient technique to address such question.

---

\* Work supported in part by the Polish State Committee grants KBN 2P03B11819 2P03B05418 and by the European Commission 5-th Framework contract HPRN-CT-2000-00149.

In general it is indispensable to divide Monte Carlo simulation into separate blocks: physics event generation and detector response. Later event generation can be divided further into parts, describing for example production and decay of the intermediate states.

In the present paper we will concentrate on the particular class of the processes involving polarised  $\tau$  leptons. The two main goals of the present paper are: (i) presentation of the algorithm for matching  $\tau$  lepton decay and its production, with some control over spin effects; in particular in case of  $Z/\gamma \rightarrow \tau^+\tau^-$  production mechanism, (ii) discussion of physical observables sensitive to the spin correlations in the  $\tau$  pair production.

Spin correlations in the decay of  $\tau$  leptons not only can help to suppress irreducible background to the possible resonant  $\tau$  pair production at LHC, such as the MSSM Higgs bosons decays, but also help to determine the spin nature of this resonance.

In the papers [1–3] TAUOLA Monte Carlo package for simulation of  $\tau$  lepton decay was described. Recently, in Ref. [4], technical details convenient for using the code in multi-purpose environment were collected, and universal interface for combining the simulation of  $\tau$  lepton decay, with different packages for generation of physics event was proposed. Scheme of Ref. [4] relies on the information stored in the HEPEVT common block [5] only, and not on the details specific for the production generator, such as PYTHIA [6] (used in our examples). In fact, such an interface can be considered as a separate software project, to some degree independent both from the specific problem of  $\tau$  production and its decay.

Our paper is organised as follows: in the next section we will describe new algorithm for extracting elementary  $2 \rightarrow 2$  body reaction for  $f\bar{f} \rightarrow Z/\gamma \rightarrow \tau^+\tau^-$ , which is necessary for properly introducing spin correlations into generation chain. In Sec. 3 we analyse spin content of such an elementary function. Sec. 4 is dedicated to the discussion of their consequences for the distributions of physics interest. In Sec. 5 we discuss few observables where spin effects can improve separation of the Higgs boson signature, in case of the 14 TeV  $pp$  collisions. Summary closes the paper. In Appendix, we explain the spin treatment used in our code. It completes the program manual given in Ref. [4].

## 2. The $\tau$ polarisation from the $Z/\gamma \rightarrow \tau^+\tau^-$ decay

The exact way of calculating spin state of any final state is with the help of the matrix element and the rigorous density matrix treatment. This is however not always possible or necessary. Often, like in the case of the production and decay of particles in the ultra-relativistic limit a simplified approach can be sufficient. Such an approach was developed for KORALZ Monte Carlo program [7] and its limitations were studied with the help of

matrix element calculations of the order  $\alpha$  [8]. In the following, we study the question whether the approach can be generalised, and the approximate spin correlation calculated from the information stored in the HEPEVT common block filled by “any”  $\tau$  production program.

The approximation consists of reconstructing information of the elementary  $2 \rightarrow 2$  body process  $e^+e^-(q\bar{q}) \rightarrow \tau^+\tau^-$ , buried inside multi-body production process. Let us stress that such a procedure can never be fully controlled, as its functioning depends on the way the production program fills the HEPEVT common block. It will be always responsibility of the user to check if in the particular case the implemented algorithm is applicable. Nonetheless our aim is *not* to replace the matrix element calculations, but rather to provide a method of calculating/estimating spin effects in cases when spin effects would not be taken care of, at all. Needless to say such an approach is limited (for the spin treatment) to the approximation not better than leading-log, and to the longitudinal spin degrees only.

The principle of calculating kinematic variables is simple. The 4-momenta of the  $2 \rightarrow 2$  body process have to be found. The 4-momenta of the outgoing  $\tau$ 's are used directly. Initial state momenta are constructed from the incoming and outgoing momenta of the particles (or fields) accompanying production of the  $Z/\gamma$  state<sup>1</sup>. We group them accordingly to fermion number flow, and ambiguous additional particles are grouped (summed) into effective quarks to minimise their virtualities. Such an approach is internally consistent in the case of emission of photons or gluons within the leading log approximation.

Longitudinal polarisation of  $\tau$  leptons  $\mathcal{P}_\tau$  depends on the spin quantum number of the  $\tau$  mother<sup>2</sup>. It is randomly generated as specified in Table I.

The probability  $P_Z$  used in the generation, is calculated directly from the squares of the matrix elements of the Born-level  $2 \rightarrow 2$  process  $f\bar{f} \rightarrow \tau^-\tau^+$ :

$$P_Z = \frac{\left| \mathcal{M} \right|_{f\bar{f} \rightarrow \tau^-\tau^+}^2(+,+)}{\left| \mathcal{M} \right|_{f\bar{f} \rightarrow \tau^-\tau^+}^2(+,+) + \left| \mathcal{M} \right|_{f\bar{f} \rightarrow \tau^-\tau^+}^2(-,-)}, \quad (1)$$

where  $f = e, \mu, u, d, c, s, b$ . It can be also expressed (following conventions of Ref. [9]), with the help of the vector (and axial) couplings of fermions to the  $\gamma$  ( and  $Z$ ) bosons. Explicit expression for the differential distributions is used. The resulting formula, given below, will be useful for the discussion of the numerical results and tests of the next sections.

---

<sup>1</sup> The  $Z/\gamma$  state does not need to be explicitly coded in the HEPEVT common block. Note that if available, information from the history part of the event, where the 4-momenta of gluons quarks *etc.* are stored, will be used.

<sup>2</sup> The spin quantisation axes are chosen *in the same way* as in Ref. [7].

TABLE I

Probability for the configurations of the longitudinal polarisation of the pair of  $\tau$  leptons from different origins.

Origin	$P_{\tau+}$	$P_{\tau-}$	Probability
Neutral Higgs bosons: $h^0, H^0, A^0$	$P_{\tau+} = +1$	$P_{\tau-} = -1$	0.5
	$P_{\tau+} = -1$	$P_{\tau-} = +1$	0.5
Charged Higgs boson: $H^+$ or $H^-$	$P_{\tau+} = +1$	$P_{\tau-} = +1$	1.0
Charged vector boson: $W^+$ or $W^-$	$P_{\tau+} = -1$	$P_{\tau-} = -1$	1.0
Neutral vector boson: $Z/\gamma^*$	$P_{\tau+} = +1$	$P_{\tau-} = +1$	$P_Z$
	$P_{\tau+} = -1$	$P_{\tau-} = -1$	$1 - P_Z$
Other	$P_{\tau+} = +1$	$P_{\tau-} = +1$	0.5
	$P_{\tau+} = -1$	$P_{\tau-} = -1$	0.5

$$P_Z(s, \theta) = \frac{\frac{d\sigma_{\text{Born}}}{d\cos\theta}(s, \cos\theta; 1)}{\frac{d\sigma_{\text{Born}}}{d\cos\theta}(s, \cos\theta; 1) + \frac{d\sigma_{\text{Born}}}{d\cos\theta}(s, \cos\theta; -1)}, \quad (2)$$

$$\begin{aligned} \frac{d\sigma_{\text{Born}}}{d\cos\theta}(s, \cos\theta; p) = & \left(1 + \cos^2\theta\right)F_0(s) + 2\cos\theta F_1(s) \\ & - p\left[\left(1 + \cos^2\theta\right)F_2(s) + 2\cos\theta F_3(s)\right]. \end{aligned} \quad (3)$$

with the four form-factors:

$$\begin{aligned} F_0(s) &= \frac{\pi\alpha^2}{2s} \left( q_f^2 q_\tau^2 + 2\text{Re} \chi(s) q_f q_\tau v_f v_\tau + \left| \chi(s) \right|^2 \left( v_f^2 + a_f^2 \right) \left( v_\tau^2 + a_\tau^2 \right) \right), \\ F_1(s) &= \frac{\pi\alpha^2}{2s} \left( 2\text{Re} \chi(s) q_f q_\tau a_f a_\tau + \left| \chi(s) \right|^2 2v_f a_f 2v_\tau a_\tau \right), \\ F_2(s) &= \frac{\pi\alpha^2}{2s} \left( 2\text{Re} \chi(s) q_f q_\tau v_f a_\tau + \left| \chi(s) \right|^2 \left( v_f^2 + a_f^2 \right) 2v_\tau a_\tau \right), \\ F_3(s) &= \frac{\pi\alpha^2}{2s} \left( 2\text{Re} \chi(s) q_f q_\tau a_f v_\tau + \left| \chi(s) \right|^2 2v_f a_f \left( v_\tau^2 + a_\tau^2 \right) \right), \end{aligned} \quad (4)$$

and

$$\chi(s) = \frac{s}{s - M_Z^2 + is\Gamma_Z/M_Z}. \quad (5)$$

Analytic expression for the coupling constants, and their numerical values are given in Table II.

TABLE II

The  $\gamma, Z$  couplings to fermions. Lowest order approximation, the numerical values are given for the effective  $\sin^2 \theta_W = 0.23147$ .

Flavour: $f$	$q_f$	$v_f$	$a_f$
Leptons: $f = e, \mu, \tau$	1	$\frac{-1+4 \sin^2 \theta_W}{4 \sin \theta_W \cos \theta_W} = -0.044$	$\frac{-1}{4 \sin \theta_W \cos \theta_W} = -0.593$
Quarks : $f = u$ or $c$	2/3	$\frac{1-(8/3) \sin^2 \theta_W}{4 \sin \theta_W \cos \theta_W} = 0.227$	$\frac{1}{4 \sin \theta_W \cos \theta_W} = 0.593$
Quarks : $f = d, s$ or $b$	-1/3	$\frac{-1+(4/3) \sin^2 \theta_W}{4 \sin \theta_W \cos \theta_W} = -0.410$	$\frac{-1}{4 \sin \theta_W \cos \theta_W} = -0.593$

In the first step of our discussion the  $\mathcal{P}_\tau$  is shown as a function of  $\cos \theta$ , for several centre of mass energies and initial state flavours. The angle  $\theta$  denotes  $\tau^-$  scattering angle in the  $Z/\gamma^*$  rest-frame. It is calculated with respect to the  $e^-, u$  or  $d$  effective beam. The  $Z$  mass  $m_Z = 91.1882$  GeV, was taken from Ref. [10], as well as effective  $\sin^2 \theta_W = 0.23147$  and  $\Gamma_Z = 2.49$  GeV.

In Fig. 1, the angular dependence of the  $\tau$  polarisation for the  $e^+e^- \rightarrow \tau^+\tau^-$  process at the peak of  $Z$  resonance and for the three different values of the centre of mass (cms) energies above it (upper plot). The  $\tau$ 's are strongly polarised in the forward direction, where polarisation approaches the value approximately twice as big as the average one (the polarisation of  $Z$  due to  $e - e - Z$  coupling sums with the one due to  $\tau - \tau - Z$  coupling). The polarisation is very small in the backward regions. For  $\cos \theta = -1$  it is equal to zero, independently of the centre of mass energy. The reason is the universality of both the  $Z$  and  $\gamma$  couplings to all leptons. As can be observed, the  $\tau$  polarisation changes significantly (especially in the forward region) with the centre of mass energy. At cms energies above the  $Z$ -peak,  $\tau$  polarisation is smaller, due to significant contribution from the  $s$ -channel  $\gamma$ -exchange — production mechanism not contributing directly to the polarisation.

Let us now turn to the production from quarks. In Fig. 1 we show the  $\tau$  polarisation for the  $u\bar{u} \rightarrow \tau^+\tau^-$  and  $d\bar{d} \rightarrow \tau^+\tau^-$  elementary processes and the same cms energies as in the previous case. For the cms energy close to the  $Z$ -peak, the  $\tau$ 's produced in the forward as well as in the backward directions are strongly polarised. The polarisation seem to be almost zero for  $\cos \theta = 0$ , but in reality is equal (nearly) to the same value as in previous case of production from electrons at  $\cos \theta = 0$ . Also, the average  $\tau$  polarisation is close to the case of production from electrons. It is, as it should be, independent from the initial state flavour, the  $Z$  was produced from. The initial state couplings of the  $Z$ , affect the angular dependence of

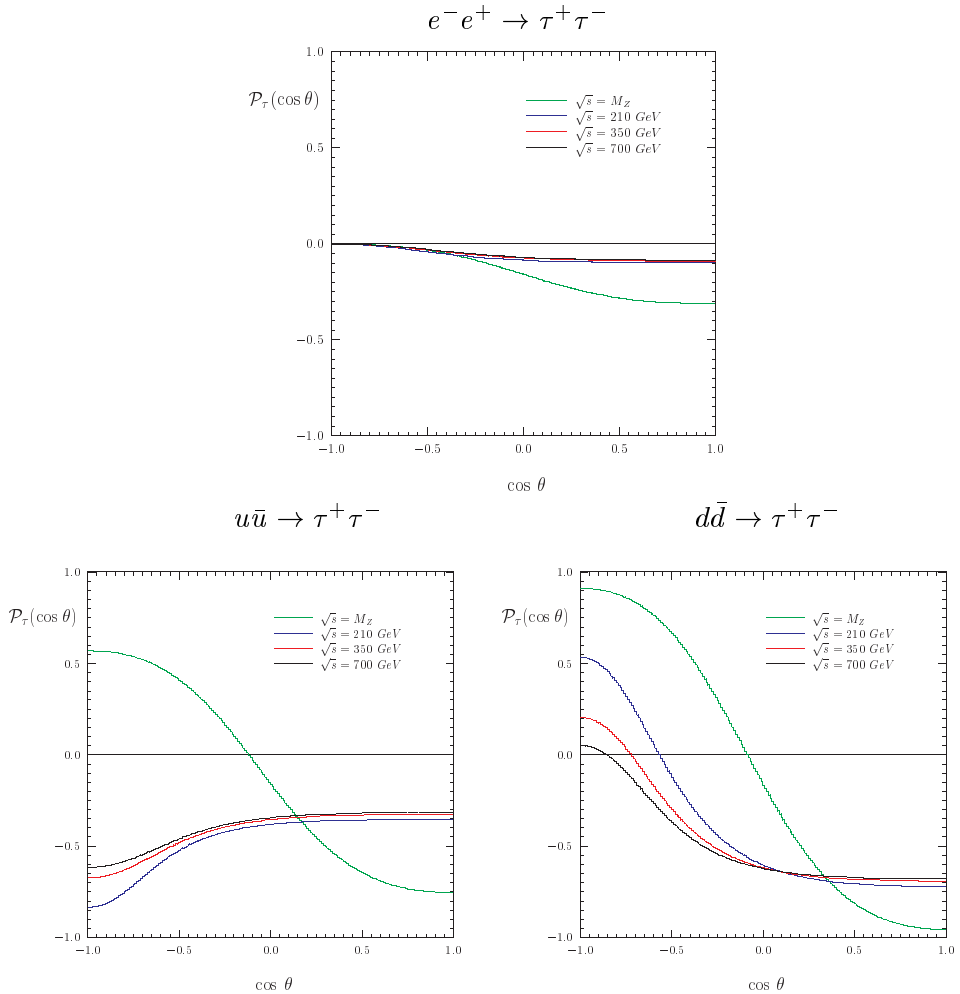


Fig. 1. Tests of the TAUOLA universal interface. The  $\tau$  lepton polarisation as a function of  $\cos\theta$ . We have used  $\sqrt{s} = M_Z, 210, 350$  and  $700$  GeV.

the  $\tau$  polarisation only, and give sizable angular asymmetry in polarisation. Obviously, the larger the initial state vector couplings to  $Z$  the larger angular dependence of the polarisation. The above arguments hold, because the contribution from the  $\gamma$  exchange is small. This is the case, in the region of the  $Z$  peak only.

Quite different polarisation pattern can be observed for quarks and cms energies far above the  $Z$  peak (see Fig. 1). Contribution from the  $\gamma$  exchange cannot be neglected. The  $\gamma - Z$  interference complicates the pattern even

more. Let us comment briefly on the numerical results. In the case of  $u$  and  $d$  initial state, polarisation is negative and nearly constant over the forward hemisphere; also the average polarisation is negative. This is because of rather large and positive forward–backward asymmetry, and polarisation forward–backward asymmetry. The average polarisation increases above the  $Z$ -peak and approaches, respectively,  $-35\%$  and  $-61\%$  in the case of  $u\bar{u}$  and  $d\bar{d}$  annihilation<sup>3</sup>. Let us point, that in the case of  $\tau$  production from the  $d$  quarks in the ultra high-energy limit, polarisation of the  $\tau$  leptons in the backward directions approaches zero (independently of the numerical value of  $\sin^2 \theta_W$ ).

### 3. Towards spin sensitive observables

Once we have understood the pattern of the  $\tau$  polarisation, let us turn to the question of its measurement. We will follow the reasoning similar to the one of Ref. [11]. The  $\tau$  polarisation  $\mathcal{P}_\tau$  can be measured from the energy distribution of its decay products. To simplify the discussion of spin effects, the decays  $\tau \rightarrow \pi\nu$  were used only<sup>4</sup>. We will compare the cases of vector  $Z/\gamma^*$  and scalar neutral Higgs boson, produced in hadron collisions and decaying into pair of  $\tau$  leptons. The  $\tau$  rest-frame cannot be accessed experimentally<sup>5</sup>, the spin effects can be seen, however, through the effects on  $\pi^+ \pi^-$  energy distributions and correlations, observed/defined for the laboratory frame.

Let us start with the following example, where for the production of the  $\tau$  lepton pairs Monte Carlo program PYTHIA was used, and for the decay Monte Carlo program TAUOLA, and our interface. It was assured, that the invariant mass of the pair of two incoming quarks was  $\sqrt{s} = m_Z = m_H$ . For the time being we discuss energies defined in the  $\tau^+ \tau^-$  pair rest-frame. With the help of variables  $z_\pm = 2E_{\pi^\pm}/\sqrt{s}$ , the spin effects are visualised. In Fig. 2 we observe the slope (as expected) of  $\pi$  energy spectrum due to  $\tau$  polarisation. The slope of the distribution is simply proportional to the polarisation (small dip at  $z_\pm \simeq 0$  is due to kinematical effect of the  $\pi$  mass)

$$\frac{d\sigma}{dz_\pm} \sim 1 + \mathcal{P}_\tau 2(z_\pm - 0.5). \quad (6)$$

---

<sup>3</sup> This may open the way for measuring the flavour of the quarks leading to  $\tau$  pair production.

<sup>4</sup> In case of the 3-body decays, such as  $\tau \rightarrow e(\mu)\nu\bar{\nu}$  sensitivity is smaller and depends on energy of leptons; in case of  $\pi \rightarrow \rho\nu$  to exploit sensitivity in full, the reconstruction of  $\pi^0$  is necessary.

<sup>5</sup> In some cases the invariant mass of  $Z/\gamma^*$  or Higgs boson, can be reconstructed from total balans of the observed transverse energies for all tracks in the event.

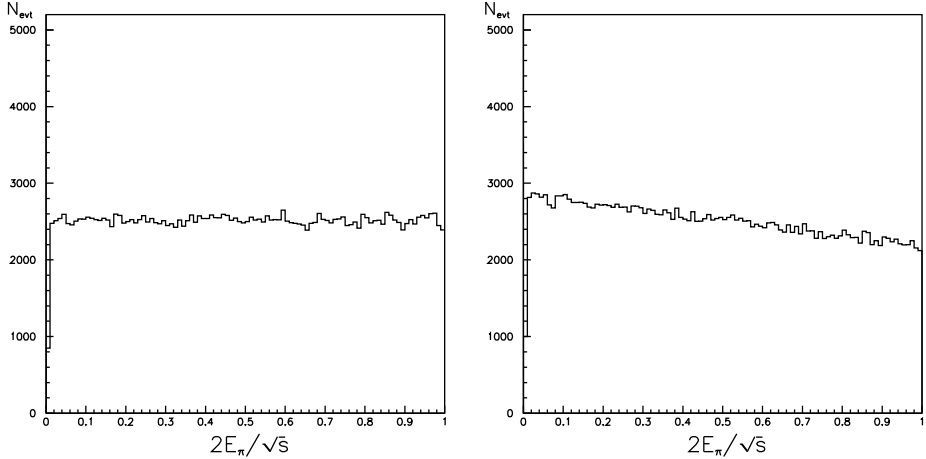


Fig. 2. Single  $\pi$  energy spectrum in the case of  $\tau$  produced from  $H$  (left-hand side) or  $Z$  (right-hand side).  $\sqrt{s} = m_H$  or  $\sqrt{s} = m_Z$  respectively. Energies are calculated in the rest frame of Higgs boson (or  $Z$ ).

In the case of the plot on the right-hand side of Fig. 2, *i.e.* decay of the  $Z$ , polarisation was about  $-14.7\%$ . In the case of the plot on the left-hand side the spectrum is flat, as would be in the case of scalar neutral Higgs boson (or pure  $\gamma$ ) where there is no polarisation.

If polarisation was  $\mathcal{P}_\tau = -100\%$ , then the distribution slope would be maximally negative and touch zero at  $z_\pm = 1$ . For  $\mathcal{P}_\tau = 100\%$ , slope would be reversed and distribution would touch zero at  $z_\pm = 0$ . These are the cases of charged Higgs boson and charged  $W$  boson decays into  $\tau\nu$ . Respective distributions are shown in Fig. 3.

Let us now turn to the question of the spin correlations. As we can see from Table I, the  $\tau$  pairs are produced with the well defined spin configurations ( $+, +$  or  $-, -$  for vector bosons;  $+, -$  or  $-, +$  for neutral Higgs boson), thus, the spin effects are to become visible on the two-dimensional distribution build on  $z_-$  and  $z_+$  variables. Indeed, for the vector bosons we expect more events when both  $\pi^+$  and  $\pi^-$  are on the upper side (case I) ( $z_+ > 0.5, z_- > 0.5$ ) or lower side (case II) ( $z_+ < 0.5, z_- < 0.5$ ), with respect to the mixed ones:  $z_+ > 0.5, z_- < 0.5$  (case III) and  $z_+ < 0.5, z_- > 0.5$  (case IV).

The appropriate asymmetry is:

$$A_{\text{FastSlow}} = \frac{\sigma_I + \sigma_{II} - \sigma_{III} - \sigma_{IV}}{\sigma_I + \sigma_{II} + \sigma_{III} + \sigma_{IV}} = 0.24. \quad (7)$$

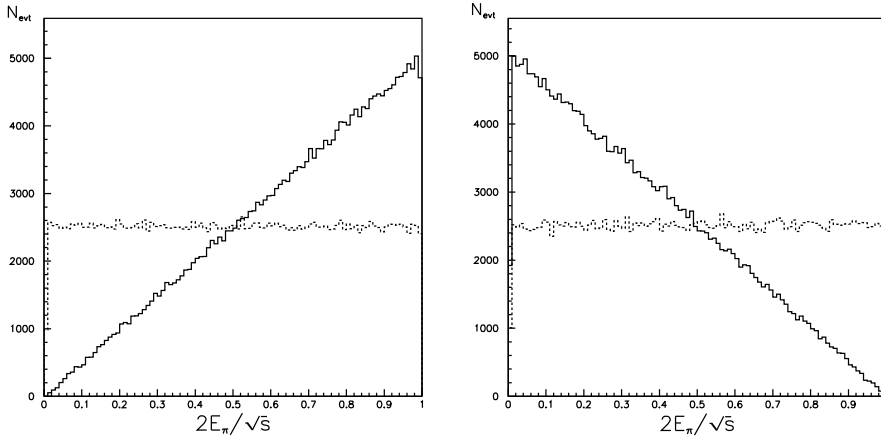


Fig. 3. Single  $\pi$  energy spectrum in the case of  $\tau$  produced from  $H^\pm$  (left-hand side) or  $W^\pm$  (right-hand side).  $\sqrt{s} = m_{H^\pm}$  or  $\sqrt{s} = m_{W^\pm}$ , respectively. Energies are calculated in the rest frame of  $H^\pm$  (or  $W^\pm$ ). Continuous line with spin effects included, dotted line with spin effects switched off.

This can be compared to the Higgs boson case, where asymmetry  $A_{\text{FastSlow}} = -0.25$ . For the Higgs boson case the  $A_{\text{FastSlow}}$  is insensitive on the choice of cms energy, as there is no interference effects at all. The sign difference is due to the vector boson nature of  $Z$ , as opposed to the scalar nature of Higgs boson.

In order to better visualise the spin correlation effect we have introduced variable  $z_s$  defined as the signed part of the following phase space part: a surface in  $z_+$ ,  $z_-$  variables between the lines  $z_+ = z_-$  and  $z_+ = z_- + a$  (the sign of  $a$  should be taken). In Fig. 4 respective plots are given for the  $H$  and  $Z$  decays. The dashed lines (which in both  $Z$  and  $H$  cases are flat) correspond to the case when spin correlations are switched off. As we expect in the  $Z/\gamma \rightarrow \tau^- \tau^+$  decays, due to spin effects a Fast (Slow)  $\pi^\pm$  is most likely associated with a Fast (Slow)  $\pi^\mp$ . The solid line has maximum at  $z_s = 0$  and approaches zero for  $z_s = \pm 0.5$ . Precisely the opposite is true in the case of  $H \rightarrow \tau^- \tau^+$ . The maximum is now at  $z_s = \pm 0.5$  and minimum for  $z_s = 0$ .

Let us now turn our attention to the quantities which (at least in principle) can be measured experimentally. Fig. 5 shows the invariant mass distribution for the case of pure  $(+, +)$  and  $(-, -)$  configurations of the  $\tau$  polarisation and the mass of the resonance equal to the  $Z$  mass. The spin correlations enhance fraction of the Fast–Fast and Slow–Slow configurations which are localised mostly at the shoulders of the  $\pi^+ \pi^-$  invariant mass distributions, the Fast–Slow configurations would be localised in the centre of the distributions.

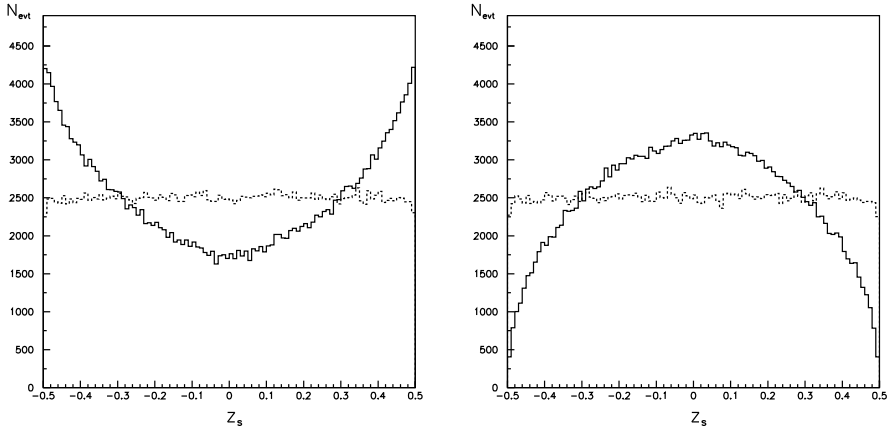


Fig. 4. Expected number of events as the function of  $z_s$  variable. Left-hand side plot for  $H$ , right-hand side for  $Z$ . Continuous line with spin effects included, dotted line with spin effects switched off.

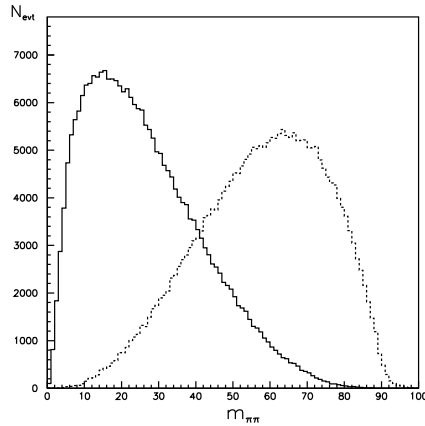


Fig. 5. The  $\pi^+\pi^-$  invariant mass distribution for  $\sqrt{s} = m_Z$ . Continuous line for pure  $(-, -)$  dotted line for pure  $(+, +)$  spin configurations.

In Fig. 6 we show  $\pi^+\pi^-$  invariant mass distribution for the Higgs boson and  $Z$  cases. Continuous line with spin effects included, dotted line with spin effects switched off. Left-hand side plot corresponds to the Higgs boson case, right-hand side to the  $Z$ . In the case of Higgs boson, the mass distribution is peaked centrally, whereas in the case of  $Z/\gamma^*$  shoulders of the distributions are more profound, especially the one at lower invariant mass additionally enhanced by the polarisation.

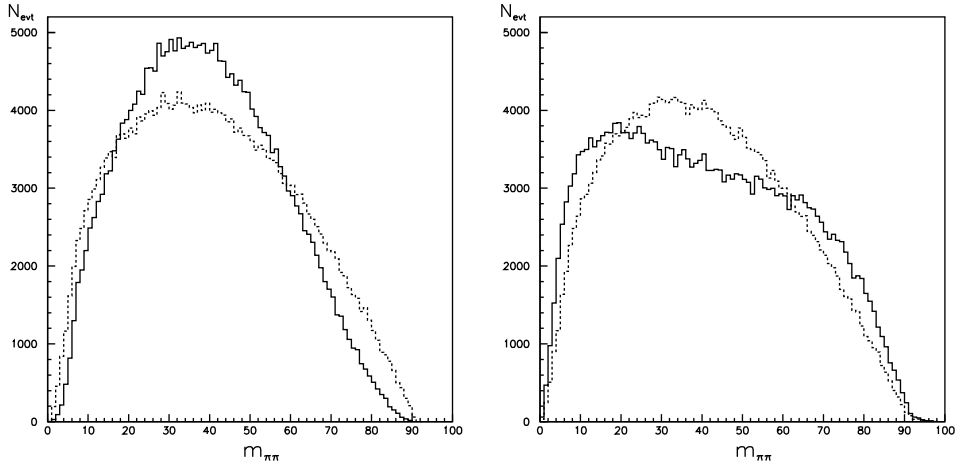


Fig. 6. The  $\pi^+\pi^-$  invariant mass distribution. Left-hand side plot for  $H$ ; right-hand side for  $Z/\gamma^*$ . Continuous line with spin effects included, dotted line with spin effects switched off. In the two cases respectively  $\sqrt{s} = m_H = m_Z$ .

For the vector case the spin correlations enhance fraction of the Fast–Fast and Slow–Slow configurations which are localised mostly at the shoulders of the  $\pi^+\pi^-$  invariant mass distributions. The relative height of the shoulders is sensitive to the average polarisation. For the scalar case, the enhancement in the fraction of the Slow–Fast configurations effects in the enhancement of the events localised in the middle of the  $\pi^+\pi^-$  invariant mass distribution, leading to the slightly narrower shape.

If all polarisation effects are switched off (dashed lines) the distributions in the two cases are identical. That observable, well defined distribution of invariant mass built from the visible decay products of the  $\tau$ 's, can be helpful in separating Higgs boson signal from the  $Z/\gamma^*$  background.

The same distribution have been also studied for the off-peak production of  $Z/\gamma^*$ , *i.e.* for the larger cms energies. In these cases the average polarisation is large and negative, also distinct for the  $u\bar{u}$  and  $d\bar{d}$  annihilation. As illustrated in Fig. 7, the effect on the  $\pi^+\pi^-$  invariant mass distribution is noticeable. The shape of the distribution might give the insight to the structure functions of the colliding protons, once the invariant mass of the  $Z/\gamma^*$  state can be reconstructed.

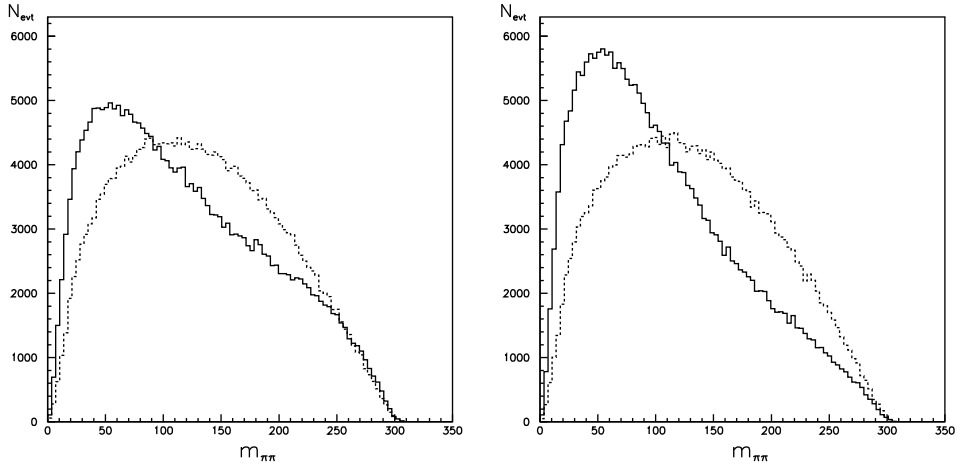


Fig. 7. The  $\pi^+\pi^-$  invariant mass distribution for  $u\bar{u} \rightarrow Z/\gamma^*$  (left-hand plot) and  $d\bar{d} \rightarrow Z/\gamma^*$  (right-hand plot) produced with cms energy of 300 GeV. Continuous line with spin effects included, dotted line with spin effects switched off.

#### 4. Case of the Higgs boson signatures at LHC

In the search for new phenomena in accelerator experiments, important parameter to estimate discovery chances is the signal sensitivity, equal to the ratio of number of expected events from the new physics divided by the square root of the expected background events. Any possible increase of such a ratio can improve chances of discovery (or improve limit of the exclusion). Use of more sophisticated cuts can be of a great help in a case when it can be combined with the physical properties of signal and/or background distributions. Equally important is the possibility for the verification of the nature of observed new physics, *e.g.* the quantum numbers of the new resonances.

The  $\tau$  leptons are considered as a very promising signature for the searches of the Higgs bosons in the Minimal Supersymmetric Standard Model (MSSM) at LHC collider [12, 13]. Below, we will briefly discuss possible applications of the discussed spin correlations in the cases of the neutral Higgs bosons  $H$  and  $A$  decay into  $\tau^+\tau^-$  pair and the charged Higgs boson  $H^\pm$  decays into  $\tau\nu$  pair.

The neutral Higgs bosons  $H$  and  $A$  decays into  $\tau^+\tau^-$  pair, are enhanced for the large values of  $\tan\beta$  ( $\tan\beta$  denotes the ratio of the vacuum expectation values of the Higgs doublets in the MSSM model), with the branching ratio of about 10% for most of the range of the interesting Higgs boson mass values (150–1000 GeV). Accessibility of the hadronic decay mode of the  $\tau^+\tau^-$  pair has been studied recently by the CMS Collaboration [14]. The

triggering on such events, signal extraction from the irreducible background  $Z/\gamma^* \rightarrow \tau\tau$  and the reducible backgrounds QCD jets,  $t\bar{t}$  and  $W + \text{jets}$ , and reconstruction of the resonance peak in the  $\tau^+\tau^-$  mass distributions seems feasible for the Higgs boson masses roughly above 300 GeV. In that study the  $\tau$  identification is based on the presence of a single hard isolated charged hadron in the jet using tracker information. The two hard tracks from  $\tau^-$  and  $\tau^+$  in the signal events have an opposite sign while no strong charged correlation is expected for the QCD jets or  $W + \text{jets}$  events. The sensitivity of  $5\sigma$  can be reached for the large fraction of the MSSM parameter space after three years of data collecting at low luminosity. The expected signal-to-background ratio is very large, being of the order of one for  $5\sigma$  sensitivity, with the background dominated by the continuum  $Z/\gamma^* \rightarrow \tau\tau$  production. The resolution for the reconstruction of the Gaussian  $m_{\tau\tau}$  peak is  $\sim 10\%$  of the mass of the Higgs boson. The above performance seems very promising but hopefully can be still improved by exploring the spin correlations and polarisations effects. The possible improvements may come from the additional suppression of the background.

But it is also important that exploring effect of the spin correlation on the invariant mass of the hadronic decay products might allow to verify hypothesis of the scalar *versus* vector nature of the observed resonance peak in the reconstructed invariant mass of the  $\tau\tau$  pair. As we have seen in the previous sections, the main difference between production mechanisms due to Higgs boson *versus*  $Z/\gamma^*$  consists of the correlation in energies of the  $\tau$  hadronic decay products.

Let us concentrate on the case of  $\tau$  decays to  $\pi\nu$  — most sensitive to the spin correlations. In Fig. 8 the  $\pi$  energy spectrum is shown in the laboratory frame for the  $H$  (left-hand side) and  $Z/\gamma^*$  (right-hand side) decays. The selection, roughly consistent with what is foreseen in the experimental analysis [12], was applied. The minimal transverse momenta of the  $\pi$ 's were required to be above 15 GeV and the pseudorapidity  $|\eta| < 2.5$ . Solid line shows results with included spin effects, dashed line with the effects switched off. Spin correlations lead to the softer spectrum of  $\pi$  in  $Z/\gamma^*$  decays, which may slightly suppress the identification efficiency of the  $\tau$  with respect to those produced from the Higgs boson decay. The slope in the distribution for the  $Z/\gamma^*$  (sensitive to the large negative average polarisation), depends also on the relative fraction of the  $u\bar{u}$  and  $d\bar{d}$  production processes simulated in the proton–proton collision, hence the parametrisation of the structure functions. Events were generated with the Monte Carlo PYTHIA 5.7 [15] and CTEQ2L structure functions; the Higgs boson mass of the 300 GeV and the width below 1 GeV (as for  $\tan\beta \sim 10$ ) was assumed. For the continuum  $Z/\gamma^*$ , the cms energy of the produced  $\tau\tau$  pair was taken in the range  $300 \pm 10$  GeV.

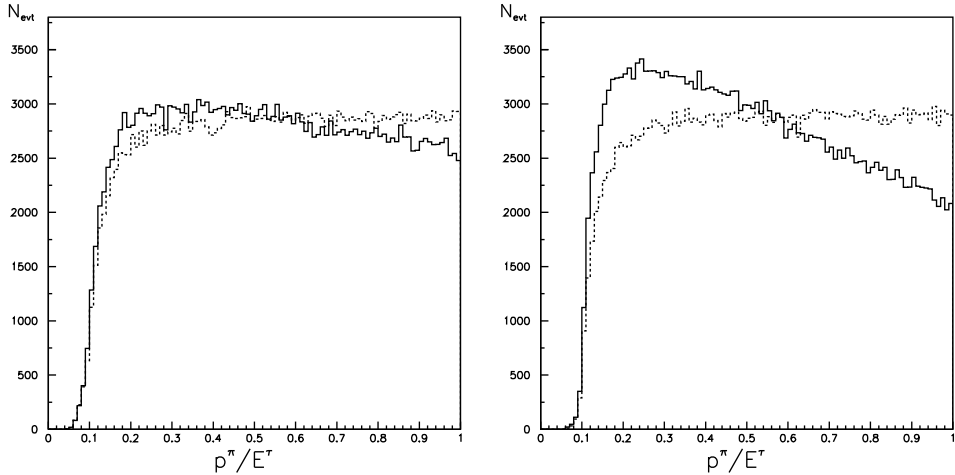


Fig. 8. The  $\pi$  energy spectrum in the laboratory frame, after basic selection as specified in text, for Higgs boson (left-hand side) and  $Z/\gamma^*$  (right-hand side). Continuous line with spin effects included, dotted line with spin effects switched off.

Fig. 9 shows the effect of the  $\pi\pi$  energy–energy correlations in the cms frame as discussed in the previous section. Although the effect seems strong enough to discriminate between scalar and vector cases, exploring this effect would require good experimental reconstruction of the effective cms frame which might be very difficult.

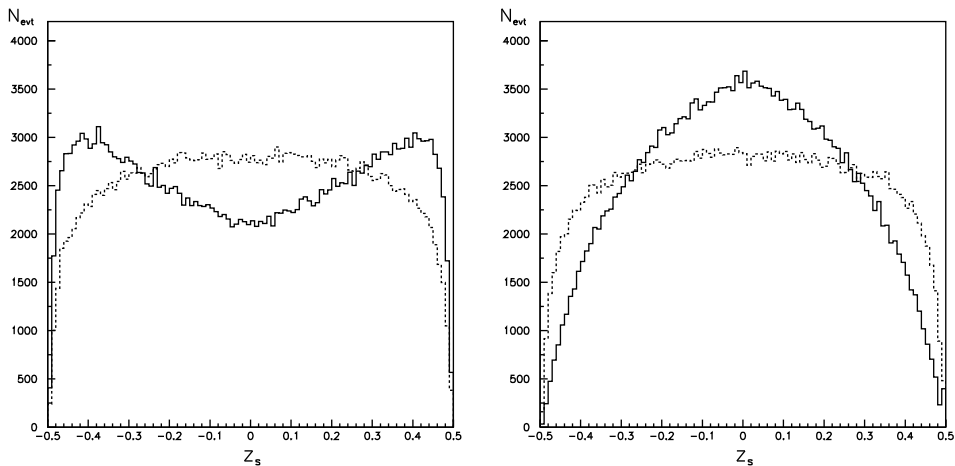


Fig. 9. The expected number of events as a function of the  $\pi^+\pi^-$  energy–energy correlation variable  $z_s$ , basic selection as specified in the text. Distributions are shown for Higgs boson (left-hand side) and  $Z^*/\gamma^*$  (right-hand side). Continuous line with spin effects included, dotted line with spin effects switched off.

The invariant mass distribution of the  $\pi\pi$  system, see Fig. 10, shows the visible effect of including spin-correlations. As discussed in the previous section, in the vector case these correlations lead to the more pronounced shoulders in the distribution and the relative height of them is sensitive to the average polarisation of the produced resonance. In the case of the scalar Higgs boson the correlations lead to the narrower distribution, enhancing fraction of events localised in its central part. With the expected signal-to-background ratio being of one or higher, this effect seems promising for determining the spin property of the studied resonance.

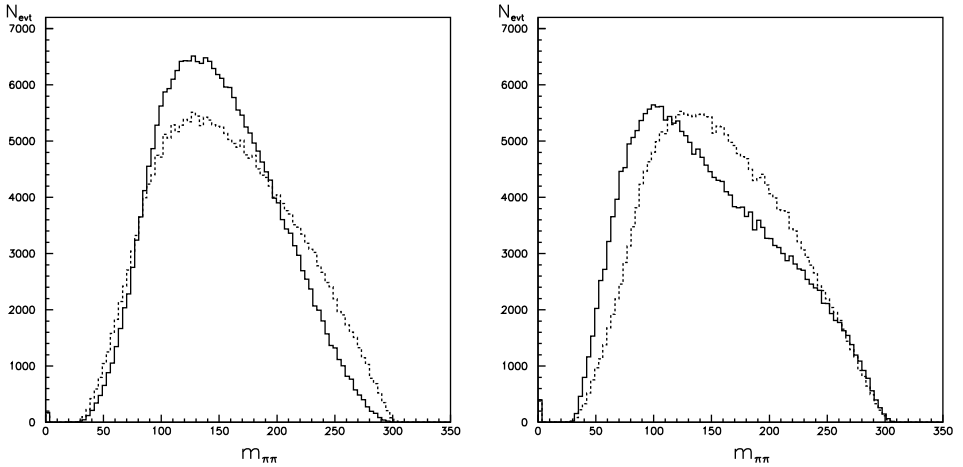


Fig. 10. The  $\pi^+\pi^-$  invariant mass distribution after basic selection. On the left for Higgs boson, on the right for  $Z/\gamma^*$ . Continuous line with spin effects included, dotted line with spin effects switched off. The Higgs boson mass was assumed to be 300 GeV (see text).

For completeness let us now turn to the case of the charged Higgs boson. The decay into  $\tau\nu$  pair is a dominant mode below the kinematical threshold of the  $t\bar{b}$  channel, and accounts for nearly 100% of cases, almost independently of  $\tan\beta$ . This branching ratio is decreasing rather rapidly above  $t\bar{b}$  threshold, but is still of the order of 10% for the Higgs boson mass of 500 GeV and large  $\tan\beta$ . The LHC detectors will be thus sensitive to signal [12, 14], with at least  $5\sigma$  significance, for Higgs boson mass up to 400–500 GeV. This sensitivity is almost independent on  $\tan\beta$  below  $t\bar{b}$  threshold. For the Higgs boson mass above top-quark mass this sensitivity is expected only for large  $\tan\beta$ . In both cases of the Higgs boson masses below and above top-quark mass, the main background comes from  $W^\pm \rightarrow \tau^\pm\nu$  decay. Harder pions are expected from the  $H^\pm$  decays than from the  $W^\pm$  decays.

The effect of the spin correlations has been already studied, theoretically in Ref. [16] and experimentally in Ref. [14]. For completeness we show in Fig. 11 the  $\pi$  energy distribution in the laboratory frame for the decays of  $H^\pm$  and  $W$  — spin effects switched on and off. The Higgs boson mass of 130 GeV was taken.

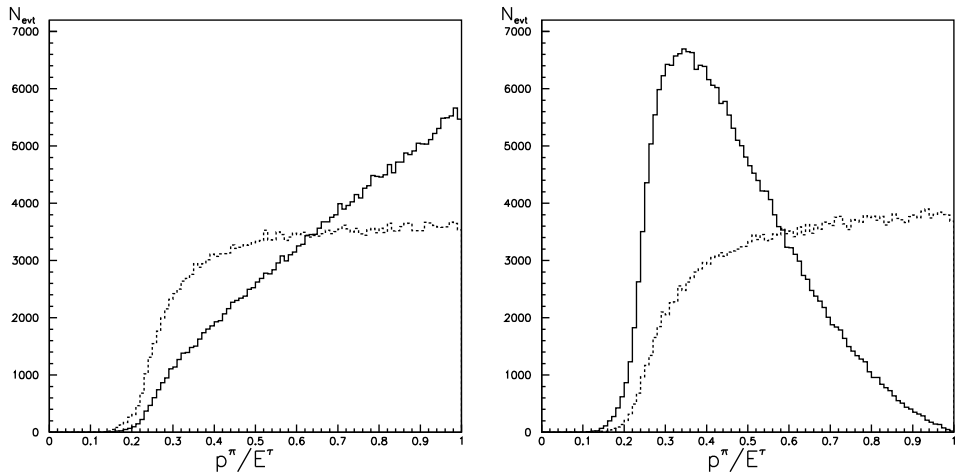


Fig. 11. Distribution of  $p^\pi/E^\tau$  after basic selection and in the laboratory frame. On the left plot for  $H^\pm$  ( $m_H = 130$  GeV), on the right for  $W^\pm$ . Continuous line with spin effects included, dotted line with spin effects switched off.

## 5. Summary

We have discussed the spin effects in the  $\tau$  pair production at LHC. A few distributions presented here, sensitive to the  $\tau^+\tau^-$  spin correlations, can be possibly used for the MSSM Higgs bosons searches scenarios at LHC to enhance sensitivity of the signal or to verify the hypothesis of the spin zero nature of the Higgs boson.

We have extended the algorithm for the interfacing the  $\tau$  lepton decay package TAUOLA with “any” production generator to include effects due to spin in elementary  $Z/\gamma^* \rightarrow \tau^+\tau^-$  process. The interface is based exclusively on the information stored in the HEPEVT common block. This code is publicly available *e.g.* from the URL address [17].

Z.W. acknowledges support of the Zürich ETH group at CERN where part of this work was done.

## Appendix A

### *Universal interface for TAUOLA package*

Let us recall first some details of the universal interface for TAUOLA and “any”  $\tau$  production generator as described in Ref. [4]. The interface uses as an input the HEPEVT common block and operates on its content only. As a demonstration example the interface is combined with the JETSET generator, however it should work in the same manner with the PYTHIA<sup>6</sup>, HERWIG or ISAJET generators as well.

The interface acts in the following way:

- The  $\tau$  lepton should be forced to be stable in the package performing generation of the  $\tau$  production.
- The content of the HEPEVT common block is searched for all  $\tau$  leptons and  $\tau$  neutrinos.
- It is checked if there are  $\tau$  flavour pairs (two  $\tau$  leptons or  $\tau$  lepton and  $\tau$  neutrino) originating from the same mother.
- The decays of the  $\tau$  flavour pairs are performed with the subroutine TAUOLA. Longitudinal spin correlations are generated in the case of the  $\tau$  produced from decay of:  $W \rightarrow \tau\nu$ ,  $Z/\gamma \rightarrow \tau\tau$ , the neutral Higgs boson  $H \rightarrow \tau\tau$ , and the charged Higgs boson  $H^\pm \rightarrow \tau\nu$ . Parallel or anti-parallel spin configurations are generated, before calling on the  $\tau$  decay, and then the decays of 100 % polarised  $\tau$ 's are executed.
- In the case of the Higgs boson (for the spin correlations to be generated) the identifier of the  $\tau$  mother must be that of the Higgs boson. Here, the particle code convention as that used by the PYTHIA 5.7 Monte Carlo is adopted.
- In case of the  $W$  and  $Z/\gamma$  it is not necessary. If from the same mother as that of the  $\tau$ , a  $\nu_\tau$  is also produced, the  $W$  is assumed as the mother of the  $\tau$ . Similarly, if from the same mother another  $\tau$  with opposite charge is produced, the  $Z/\gamma$  is assumed to be the mother of the  $\tau$  pair.
- Photon radiation in the decay is performed with PHOTOS package [18, 19].
- Let us note that the calculation of the  $\tau$  polarisation created from the  $Z$  and/or virtual  $\gamma$  (as function of the direction) represents a rather non-trivial extension. Generally, the dedicated study of the production matrix elements of the host generator is necessary in every individual case.

---

<sup>6</sup> It was already checked to be the case.

For some of the technical details on how to use the interface we address the reader to Ref. [4]. For general documentation of TAUOLA to Ref. [1–3]. For the use of PYTHIA reference to [15] and references therein will be the best.

Here, let us concentrate on practical details. The TAUOLA interface is organised in a modular form to be used conveniently in “any environments”.

### Initialisation

Initialisation is performed with the CALL TAUOLA(MODE,KEYSPIN), MODE=-1. All necessary input is directly coded in subroutine TAUOLA placed in a file `tauface-jetset.f`.

The following input parameters are set at this call (we omit those which are standard input for TAUOLA as defined in its documentation). They are hard-coded in the subroutine.

Parameter	Meaning
POL	Internal switch for spin effects in $\tau$ decay. Normally the user should set POL=1.0, and when POL=0.0 spin polarisation effects in the decays are absent
KFHIGGS(3)	(KF=25, 35, 36) Flavour code for $h$ , $H$ and $A$
KFHIGCH	(KF=37) Flavour code for $H^+$
KFZO	(KF=23) Flavour code for $Z^0$
KFGAM	(KF=22) Flavour code for $\gamma$
KFTAU	(KF=15) Flavour code for $\tau^-$
KFNUE	(KF=16) Flavour code for $\nu_\tau$

### Event generation

For every event generated by the production generator, all  $\tau$  leptons will be decayed with the single CALL TAUOLA(0,KEYSPIN), (KEYSPIN=1/0 denotes spin effects switched on/off). Then, all  $\tau$  leptons, will be first localised, their positions stored in internal common block TAUPOS, and the information necessary for calculation of  $\tau$  spin state will be read in, from HEPEVT common block. Later spin state for the given  $\tau$  (or  $\tau$  pair) will be generated, and finally decay of polarised  $\tau$  will be performed with the standard TAUOLA action. In particular, the decay products of  $\tau$  will be boosted to the laboratory frame and added to the complete event configuration stored in HEPEVT common block.

### Calculation of the $\tau$ spin state

Once `CALL TAUOLA(0,KEYSPIN)` is executed and  $\tau$  leptons found, the spin states need to be calculated.

First, we look in `HEPEVT` for the position of  $\tau$ 's mothers, and store them, in matrix `IMOTHER(20)`. Each mother giving  $\tau$  lepton(s) is stored only once, independently of the number of produced  $\tau$ 's. Later, for every `IMOTHER(i)` we execute the following steps:

- The daughters which are either  $\tau$  leptons, or  $\nu_\tau$  are searched for.
- Daughters are combined in pairs, case of more than 1 pair is not expected to be important and ad hoc pairing is then performed.
- The two main cases are thus  $(\tau \tau)$  or  $(\tau \nu)$ .
- The default choices are, respectively,  $Z/\gamma$  or  $W$ , unless the identifier of `IMOTHER(i)` is explicitly that of neutral (or charged) Higgs boson.
- Calculation of the spin parameters is kinematics independent and straightforward in all cases except  $Z/\gamma$  (see Sec. 2 for details on physics).
- For  $Z/\gamma$ , the  $P_Z$  is calculated with the help of the function `PLZAPX(HOPE,IMO,NP1,NP2)`. The `HOPE` is the logical parameter defined in subroutine `TAUOLA` placed in file `tauface-jetset.f`. It tells whether spin effects can be calculated or not. It is set to `.false.`, if available information is incomplete, then, `PLZAPX(HOPE,IMO,NP1,NP2)` returns 0.5. The `IMO` denotes position of the  $\tau$  mother in `HEPEVT` common block `NP1` position of  $\tau^+$  and `NP2` of  $\tau^-$ .
- To calculate reduced  $2 \rightarrow 2$  body kinematical variables  $s$  and  $\cos\theta$  subroutine `ANGULU(PD1,PD2,Q1,Q2,COSTHE)` is used. 4-momenta of the incoming effective beams and outgoing  $\tau^+$  and  $\tau^-$  are denoted by `PD1,PD2,Q1,Q2`, respectively.

### Run summary

After the series of events is generated, the optional `CALL TAUOLA(1,KEYSPIN)` can be executed. The information on the whole sample, such as number of the generated  $\tau$  decays, branching ratios calculated from matrix elements *etc.*, will be printed.

### Demonstration program

Our main program `demo.f` is stored in subdirectory `demo-jetset`. It reads in the file `init.dat` which includes some input parameters for the particular run, such as number of events to be generated (by `JETSET/PYTHIA`), or the type of the interaction it should use to produce  $\tau$ 's, *etc.* We address the reader directly to the code for more details. It is self-explanatory.

## REFERENCES

- [1] S. Jadach, J.H. Kühn, Z. Wąs, *Comput. Phys. Commun.* **64**, 275 (1990).
- [2] M. Jezabek, Z. Wąs, S. Jadach, J.H. Kühn, *Comput. Phys. Commun.* **70**, 69 (1992).
- [3] R. Decker, S. Jadach, J.H. Kühn, Z. Wąs, *Comput. Phys. Commun.* **76**, 361 (1993).
- [4] P. Golonka, E. Richter-Was, Z. Wąs, [www.arXiv.org/abs/hep-ph/0009302](http://www.arXiv.org/abs/hep-ph/0009302).
- [5] Particle Data Group, C. Caso *et al.*, *Eur. Phys. J.* **C3**, 1 (1998).
- [6] T. Sjöstrand, *Comput. Phys. Commun.* **82**, 74 (1994).
- [7] S. Jadach, B.F.L. Ward, Z. Wąs, *Comput. Phys. Commun.* **79**, 503 (1994).
- [8] Z. Wąs, *Acta Phys. Pol.* **B18**, 1099 (1987).
- [9] P. H. Eberhard *et al.*, Proceedings of the Workshop on Z Physics at LEP, edited by G. Altarelli, R. Kleiss and V. Verzegnassi, CERN-89-08 v.1-3, Switzerland, Geneva 1989.
- [10] Particle Data Group, D.E. Groom *et al.*, *Eur. Phys. J.* **C15**, 1 (2000).
- [11] S. Jadach, Z. Wąs, *Acta Phys. Pol.* **B15**, 1151 (1984); Erratum *Acta Phys. Pol.* **B16**, 483 (1985).
- [12] ALEPH Collaboration, CERN-LHCC/99-15.
- [13] CLEO Collaboration, CERN-LHCC/94-44.
- [14] R. Kinnunen, D. Denegri, CMS Note 1999/037.
- [15] T. Sjostrand *et al.*, [www.arXiv.org/abs/hep-ph/0010017](http://www.arXiv.org/abs/hep-ph/0010017).
- [16] D.P. Roy, *Phys. Lett.* **B459**, 607 (1999).
- [17] [www.home.cern.ch/~wasm](http://www.home.cern.ch/~wasm).
- [18] E. Barberio, B. van Eijk, Z. Wąs, *Comput. Phys. Commun.* **66**, 115 (1991).
- [19] E. Barberio, Z. Wąs, *Comput. Phys. Commun.* **79**, 291 (1994).